Modes of counterion density fluctuations and counterion-mediated attractions between like-charged fluid membranes

Bae-Yeun Ha
Department of Physics, Simon Fraser University, Burnaby, British Columbia, Canada V5A 1S6
(Received 15 September 2000; revised manuscript received 17 May 2001; published 30 August 2001)

Counterion-mediated attractions between like-charged fluid membranes are long ranged and nonpairwise additive at high temperatures. At low temperatures, however, they are pairwise additive, and decay exponentially with the membrane separation. Using a simple model for the electrostatic attraction between like-charged surfaces, we show that the nature of these attractions is determined by the dominant modes of fluctuations in the density of counterions. While the nonpairwise additive interactions arise from long-wavelength fluctuations and vanish at zero temperature, the short-ranged pairwise additive interactions arise from short-wavelength fluctuations and are stronger at low temperatures.

DOI: 10.1103/PhysRevE.64.031507 PACS number(s): 61.20.Qg, 05.70.Np

I. INTRODUCTION

Counterion-mediated attractions play a significant role in many physical and biological phenomena [1–11]. The classic example is DNA packaging in bacteriophages [5,6]. These attractions are also responsible for the formation of microtubule-actin bundles, which control the shape and movement of cells [7]. These attractions can also be crucial in promoting adhesion and fusion of biological membranes [12]. Another important, but less understood, example is the stabilization of cell membranes against rupture by multivalent counterions [13]. Accordingly, significant effort has been expended in developing a practical way of investigating the nature of counterion-mediated attractions. In addition to an integral equation method [14], two distinct approaches have emerged. The first approach [15,16], based on a fluctuation picture, suggests that attractions are mediated by correlated fluctuations of ion clouds of counterions. This approach is consistent with our conception of counterions as fluctuating objects, and thus merits significant consideration [1,2,4,8,9]. In the second approach, based on a zero temperature picture [17–21], the appearance of the attractions is attributed to the strong structural charge correlations that drive the systems, together with counterions, into an ionic crystal. Due to its simplicity, this approach was also used extensively [17–21]. At first glance these two approaches appear to be contradictory to one another, but there is some evidence that they can, in fact, be complimentary [22–24]. Despite this, there still remain fundamental discrepancies between the two that have yet to be resolved [25]. For the case of two planar surfaces a distance h apart, the charge-fluctuation approach leads to an attractive force that scales as h^{-3} [8,9], as long as h is sufficiently large. In the zero-temperature picture, however, the attraction decays exponentially with h [17]. Furthermore, when applied to many rod systems [2,23,26], the charge-fluctuation approach suggests that interactions between rods are not pairwise additive, while the exponentially decaying interactions between plates as implied by the zero-temperature approaches are pairwise additive. A unified description of these attractions has so far been lacking [27].

Inspired by the gap between the two existing theories, we present a simple model for electrostatic attractions between like-charged surfaces. First of all, we must emphasize that there is no way to reconcile the two completely, since the regimes they represent are separated by a phase transition, i.e., crystallization. To avoid this difficulty, we restrict ourselves to the regime above the freezing temperature [28]. Even in this case, there exists a short-range attraction arising from structural correlations as will be detailed later. To this end, we use an approximate model [see Eq. (2)], which is similar in spirit to the previous modes first proposed in Ref. [22], that can approximately capture the essential physics transparent in both cases; our theory recognizes low-temperature ordering as a phase dominated by charge fluctuations at short-length scales, rather than an ionic crystalline phase below the freezing temperature. This is invoked by the fact that charge correlations decay monotonically at high temperatures, and cross over to oscillatory decays as the temperature decreases. Eventually the decay length diverges at the spinodal to an ionic crystal—this is where the high-temperature ''liquidlike'' phase becomes unstable to the formation of an ionic crystal. While monotonically decaying correlations are driven by thermal fluctuations, oscillatory correlations mainly arise from charge fluctuations at short length scales and are reminiscent of low-temperature ordering, since their amplitude increases as the temperature is lowered. However, it should be noted that our calculations may not provide much insight into the nature of counterion ordering at too low temperatures. While a complete approach is not available, our calculations can form a first step toward filling the gap between the existing approaches [27], and stimulate further investigation into this highly nontrivial problem. The main advantage of our approach lies in that it is well suited to many-plate systems and can easily be generalized to rodlike systems such as DNA and other highly charged polyelectrolytes. It also allows one to study charge correlations systematically.

Using our model, we show that the nature of the attractions is controlled by the dominant modes of fluctuations in the density of counterions. At high temperatures, the attractions are dominated by long-wavelength fluctuations, and are long ranged and nonpairwise additive. In this case, in-plane charge correlations decay algebraically in space. As the tem-

perature decreases, the high-temperature behavior crosses over to one determined mainly by short-wavelength fluctuations, as characterized by in-plane charge correlations that are oscillatory. The resulting interactions decay exponentially in space, and are approximately pairwise additive. Finally we obtain a phase diagram to depict the two distinctive regimes characterized by the corresponding dominant modes.

II. MODEL AND FREE ENERGY

The system we consider here consists of N negatively charged parallel membranes with neutralizing counterions, assumed to be localized in the plane of the membrane. The main purpose of the present work is to study the crossover from the high-temperature results for the membrane attractions to the behavior expected at low temperatures. Since this crossover occurs at low temperatures or at high densities of counterions, the assumption of localized counterions is reasonable. Thus this approximation inevitably leaves out discussions about the appearance of a short-distance regime of $1/h$ pressure for $h \ll \lambda$, arising from delocalized counterions [9,10,29]. The charge distribution on a layer j is described by the local surface charge density, $\hat{\sigma}_j(\mathbf{r}_\perp) = -em_1 + em_2 Z$, where e is the electronic charge, $m_1, m_2 = 0,1,2,3,...$ are the number of backbone charges and counterions per unit area at $\mathbf{r}_\perp \equiv (x,y)$, respectively and Z is the counterion valency. The interaction Hamiltonian is simply

$$\mathcal{H} = \frac{1}{2\epsilon} \sum_{ij=1}^{N} \int \int d\mathbf{r}_\perp d\mathbf{r}'_\perp \frac{\hat{\sigma}_i(\mathbf{r}_\perp)\hat{\sigma}_j(\mathbf{r}'_\perp)}{\sqrt{(\mathbf{r}_\perp - \mathbf{r}'_\perp)^2 + h_{ij}^2}}, \qquad (1)$$

where ϵ is the dielectric constant of the solvent, and h_{ij} is the separation between plates i and j. Here we use two-dimensional Debye-Hückel (DH) theory for systems of ions with internal structures, i.e., charge correlations over the ionic size D, as in Refs. [22–24]. It should be noted that DH theory for point charges fails to capture the strong charge correlations at low temperatures. This defect in the DH theory has been corrected in an approximate way by taking into account short-ranged charge correlations over the size of ions [22–24]. We thus implement DH theory with counterion size via the two-dimensional form factor $g(\mathbf{r}_\perp, \mathbf{r}'_\perp) = \Theta(|\mathbf{r}_\perp - \mathbf{r}'_\perp| - D)/\pi D^2$, where D is the diameter of the counterions. This is to capture the discrete nature of ions in the continuum description of charge fluctuations and thus to ensure finite charge separation at low T that the DH theory for point charges suppresses, where T is the temperature. However, it should be noted that this remedy does not naturally give rise to a hard core repulsion between the plates, since it ignores the ionic size perpendicular to the surface. Further consideration of the nonzero ionic size is thus certainly warranted. Neverthless, this approach led to charge correlations in qualitative agreement with known results, when applied to an electrolyte solution consisting of positively and negatively charged spheres [22].

The major difference between the approach we adopted here and the one used in the zero temperature approach [17,21] is that we put positive and negative ions on an equal footing, as is the case for fluid membranes. On the other hand, the (negative) backbone charge is assumed to be uniformly smeared out in the latter—it is only counterions that give rise to charge fluctuations. In our approach, the finite size effect is crucial in ensuring finite-charge fluctuations at low temperatures. In contrast, counterions can crystallize in the latter case even if counterions are pointlike. However, it should be noted that the backbone charge is treated differently there. This may make the comparison between the two obscure. Despite this, the exponentially decaying attraction, as supported by the zero-temperature picture, is a generic feature of counterions mediated attractions at low temperatures, even though the precise dependence of the strength on the temperature can be model specific. In fact, in-plane charge correlations should oscillate at low temperatures no matter what model is used. In Appendix A, we argue that the attraction decays exponentially as long as the in-plane charge correlation oscillates. The main purpose of this paper is to discuss how these distinct behaviors of the electrostatic pressure arise, rather than to attempt to completely reconcile the two exsisting approaches, i.e., the fluctuation and zero-temperature approaches. Nor do we explore the role of crystallization in determining the electrostatic attraction.

We find that the charge-fluctuation contribution to the free energy per area is [31]

$$\frac{\Delta F_N}{k_B T} = \frac{1}{2} \int \frac{d\mathbf{k}_\perp}{(2\pi)^2} \left\{ \log[\det Q(\mathbf{k}_\perp)] - N \frac{g(\mathbf{k}_\perp)}{\lambda k_\perp} \right\}, \qquad (2)$$

where $\lambda^{-1} \equiv 2\pi(1+Z) l_B \sigma_0$ estimates the strength of charge fluctuations, $-e\sigma_0$ is the surface charge density, and $l_B = e^2/\epsilon k_B T$ is the Bjerrum length, i.e., the length scale at which the electrostatic energy between two charges is comparable to the thermal energy. The matrix $Q(\mathbf{k}_\perp)$ is defined by the matrix elements

$$Q_{ij}(\mathbf{k}_\perp) = \delta_{ij} + \frac{g_{ij}(\mathbf{k}_\perp)}{\lambda k_\perp} e^{-k_\perp h_{ij}}, \qquad (3)$$

where $g_{ij}(\mathbf{k}_\perp)$ is $g(\mathbf{k}_\perp) \equiv [2J_1(k_\perp D)/k_\perp D]$ if $i=j$ and 1 otherwise, and $J_1(x)$ is the first-order Bessel function of the first kind.

First note that the free energy of an N-plate system is not simply a pairwise sum of the corresponding two-plate results over all pairs of plates. Thus pairwise additivity is not *always* satisfied. For the $N=2$ case, our result in Eq. (2) reduces to the previous two-plate result (see Eq. 3 of Ref. [9]), if D is set to zero. If we set D to zero, the free energy has a single minimum at a nonzero value $k_\perp = k_\perp^< \ll 1$ Å^{-1} for all values of λ. The dominance of the long-wavelength charge fluctuations is responsible for the breakdown of pairwise additivity of electrostatic interactions between macroions. It has been shown that pairwise additivity for the case of charged rods breaks down if the expansion of the corresponding interaction free energy in powers of l_B diverges [1,2,23]. For rod systems, the free energy is dominated by the zero-k mode, and thus this expansion converges *only when* the charge fluctuation along the rods is sufficiently small. The convergence of the l_B expansion can be tested by estimating $\delta \equiv (k_\perp^<)^{-1}\lambda^{-1}$; the l_B expansion is convergent if $\delta < 1$. How-

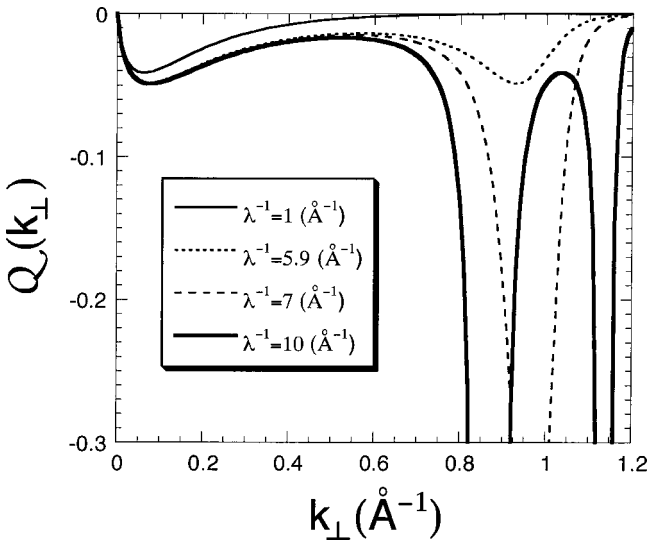

FIG. 1. The free energy between two plates separated by $h=5$ Å, as a function of $k_\perp$. We have chosen $D=5$ Å. When $\lambda^{-1}=1\ \text{Å}^{-1}$, the free energy has only one minimum at $k_\perp \ll 1\ \text{Å}^{-1}$, while when $\lambda^{-1}=5.9\ \text{Å}^{-1}$ the free energy has another local minimum at $k_\perp=k_\perp^{>}=O(1\ \text{Å}^{-1})$. When $\lambda^{-1}=7\ \text{Å}^{-1}$, the second minimum at large $k_\perp$ is overwhelmingly dominant. When $\lambda^{-1}=10\ \text{Å}^{-1}$ the free energy has two local minima at $k_\perp=O(1\ \text{Å}^{-1})$.

ever, we find that δ is smaller for smaller values of λ^{-1} and is comparable to unity if $\lambda^{-1}<10^{-3}$. Thus the pairwise additivity can easily be violated in two-dimensional systems, as in one-dimensional cases.

A. Two-plate case

At low T or at high σ_0, it is crucial to incorporate $D\neq 0$ [22–24]. To examine the low-T behavior of the free energy (thus with D set to a finite value), we consider the following quantity: $Q(\mathbf{k}_\perp)\equiv k_\perp \log[\det Q(\mathbf{k}_\perp)]$ for $N=2$, i.e., the first term in {...} of Eq. (2) for $N=2$ multiplied by $k_\perp$. In Fig. 1, we plot this quantity $Q(\mathbf{k}_\perp)$ as a function of $k_\perp$ for several different values of λ. We have chosen $D=5$ Å and $h=5$ Å. When $\lambda^{-1}=1\ \text{Å}^{-1}$, $Q(\mathbf{k}_\perp)$ has a single minimum at $k_\perp=k_\perp^{<}\ll 1$. This implies that the free energy is dominated by long-wavelength charge fluctuations as in the previous case of point charges. We find that the function $Q(\mathbf{k}_\perp)$ has two minima at $k_\perp=k_\perp^{<}\ll 1\ \text{Å}^{-1}$ and at $k_\perp=k_\perp^{>}=O(1\ \text{Å}^{-1})$, respectively, for $\lambda^{-1}>4.2\ \text{Å}^{-1}$ (not shown in the figure). As λ^{-1} changes, the minimum at $k_\perp=k_\perp^{>}$ varies monotonically, and is deeper for larger λ^{-1}. The minimum at $k_\perp=k_\perp^{<}$, however, is roughly independent of λ. When $\lambda^{-1}\approx 5.9\ \text{Å}^{-1}$, the two minima are comparable in magnitude. When $\lambda^{-1}=7\ \text{Å}^{-1}$, the function $Q(\mathbf{k}_\perp)$ is overwhelmingly dominated by the second minimum at $k_\perp=k_\perp^{>}$, as shown in the figure.

At $\lambda^{-1}=\lambda_X^{-1}\simeq 7.2\ \text{Å}^{-1}$, the second minimum diverges. This is suggestive of the onset of crystallization of counterions, where the high-T liquidlike phase is unstable to the formation of an ionic crystal. However, our theory does not accurately describe the system near *and* beyond this point. Already transparent within our theory are the existence of a crossover from the high-T regime to one dominated by short-wavelength fluctuations, *and* the interplay between the dominant modes of charge fluctuations and the nature of the corresponding interactions [see Eq. (4)]. Thus in this paper we do not attempt to accurately capture the effect of low-T ordering on the membrane interactions, and may leave out many subtle features of low-T ordering below the freezing transition [28]. Even though the region $\lambda^{-1}\geqslant\lambda_X^{-1}$ is certainly beyond the validity of our theory, it is nevertheless interesting to see what our theory implies for that region. Notably, the free energy curve corresponding to $\lambda^{-1}=10\ \text{Å}^{-1}$ has two local minima at large $k_\perp=O(1\ \text{Å}^{-1})$. The existence of multiple minima at large $k_\perp$ assures that the system is in a solidlike phase.

Our results in Fig. 1 imply that there are two distinct contributions to the free energy: long-wavelength (LW) fluctuations and short-wavelength (SW) fluctuations in the density of counterions. They also imply that the SW fluctuation contribution to the free energy has a much narrower peak if $\lambda^{-1}\gg 5.9\ \text{Å}^{-1}$. This enables us to separate the SW contribution from the LW contribution. By noting that $e^{-k_\perp h}$ does not change appreciably over the region inside the peak at $k_\perp=k_\perp^{>}$, we find, up to h-independent terms,

$$\Delta F_2 \simeq -\frac{k_B T}{16\pi}\frac{\zeta(3)}{h^2}-\frac{k_B T}{8\pi^2}\frac{e^{-2k_\perp^{>}h}}{\lambda^2}\times\int_{k_\perp\simeq k_\perp^{>}}\frac{k_\perp^{-1}dk_\perp}{[1+k_\perp^{-1}\lambda^{-1}g(k_\perp)]^2}, \tag{4}$$

where $\zeta(x)$ is the zeta function [thus $\zeta(3)/16\pi\simeq 0.024$].

The first term denoted by $F_{\rm LW}$ is the free energy calculated with D set to zero [8–10,33] and is the LW free energy. Our previous analysis on $Q(\mathbf{k}_\perp)$ implies that the SW free energy denoted by $F_{\rm SW}$, i.e., the second term in Eq. (4), is dominant over $F_{\rm LW}$ at low temperatures ($\lambda^{-1}\gg 5.9\ \text{Å}^{-1}$), and decays exponentially in space. This exponentially decaying interaction is analogous to the previous zero-T result [17]. There can, however, be ambiguity in drawing such an analogy; our model treats backbone charges, and their counterions on an *equal* footing, while the zero-T approach considers counterions confined on a uniformly charged surface. Despite this, the exponential decay appears to be a universal feature of the attraction at low T, though the prefactor can be model dependent (also see Appendix A). At high temperatures corresponding to $\lambda^{-1}\ll 5.9\ \text{Å}^{-1}$, however, the free energy is mainly determined by $F_{\rm LW}$. In this case, the fluctuation contribution to the pressure between the two plates scales as $-h^{-3}$ [8–10,33]. Also note that this LW contribution vanishes at $T=0$. This follows from the fact that $Q(k_\perp^{<})$ is roughly independent of λ. To estimate the temperature dependence of $F_{\rm SW}$, note that the prefactor of this term varies as T^{-1}. The $k_\perp$ integral of this term depends on the depth and width of the second minimum of $Q(k_\perp)$ at $k_\perp=k_\perp^{>}$. While the width is roughly independent of λ for given h, the minimum becomes deeper with the increasing λ^{-1} (or decreasing T). This proves that $F_{\rm SW}$ is more negative at low T

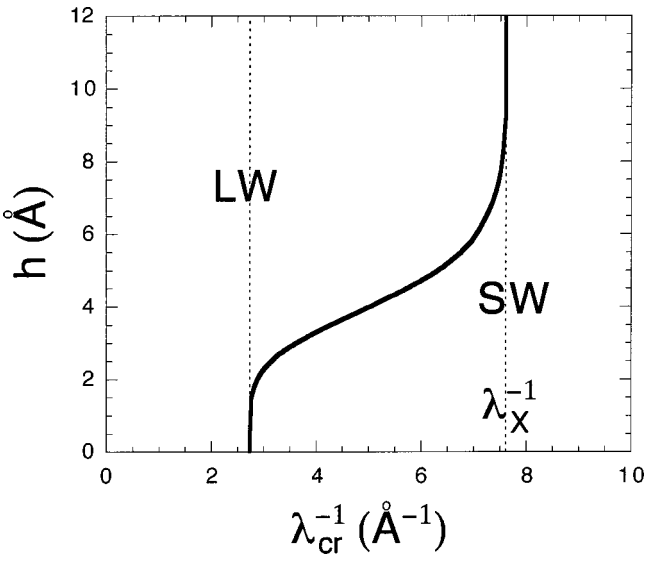

FIG. 2. Phase diagram for two plates. The regimes where long- and short-wavelength fluctuations dominate are denoted by LW and SW, respectively. Only when $2.7\,\text{Å}^{-1} \leqslant \lambda^{-1} \leqslant 7.6\,\text{Å}^{-1}$, the crossover between the two regimes takes place for a finite value of h. At $\lambda^{-1}=2.7\,\text{Å}^{-1}$, marked by the vertical dotted line on the left, the SW contribution vanishes, while the LW term becomes vanishingly small at λ_X^{-1}, marked by the vertical dotted line on the right. These results suggest that the SW fluctuations solely determine the plate interaction beyond $\lambda_X^{-1} \simeq 7.6\,\text{Å}^{-1}$, but this region is beyond the validity of our theory and should not be taken literally.

than at high T, as opposed to F_{LW}.

B. Crossover from high-T to low-T behaviors

For a given value of h, there exists a special value λ_{cr} at which the crossover between F_{LW} and F_{SW} takes place. By requiring $(\partial/\partial h)(F_{\text{LW}}-F_{\text{SW}})=0$, we have the following transcendental equation for λ_{cr}:

$$\left(\frac{\pi}{2}\right)\frac{\zeta(3)}{k_\perp^>}\,\frac{e^{2k_\perp^> h}}{h^3}\,\frac{1}{\lambda_{cr}^2}\int_{k_\perp \simeq k_\perp^>}\frac{k_\perp^{-1}dk_\perp}{[1+k_\perp^{-1}\lambda_{cr}^{-1}g(k_\perp)]^2}. \quad (5)$$

To solve the transcendental equation, we have chosen $D=5$ Å Figure 2 describes distinct regimes characterized by the corresponding dominant modes of fluctuations, and the crossover boundaries between them; the regimes where the LW and SW fluctuations dominate are denoted by LW and SW, respectively. When λ^{-1} is smaller than 2.7 Å^{-1}, the plate interaction is solely determined by the LW fluctuations for the whole range of h. At $\lambda^{-1}\simeq 2.7\,\text{Å}^{-1}$, marked by the vertical dotted line on the left, the SW fluctuations start to contribute to the plate interaction. When $2.7\,\text{Å}^{-1}\leqslant\lambda^{-1}\leqslant 7.6\,\text{Å}^{-1}$, however, the plate interaction is determined by the competition between the two; the crossover from the LW to SW regime takes places for larger value of h at low temperatures (corresponding to larger λ^{-1}). Our theory implies that the SW fluctuations solely determine the plate interaction beyond $\lambda_X^{-1}\simeq 7.6\,\text{Å}^{-1}$ [32], but this region is beyond the validity of our theory and warrants further consideration.

III. ASYMPTOTIC ANALYSIS OF THE FREE ENERGY: N-PLATE CASE

We have shown that the nature of counterion-mediated attractions between two like-charged plates is dictated by the dominant modes of counterion-density fluctuations. We now consider a system of N-parallel plates that are equally spaced, i.e., $h_{ii+1}\equiv h$. The nature of interactions between plates also depends on the dominant modes of charge fluctuations as in two-plate cases. At high temperatures, the free energy is dominated by LW fluctuations. In this case, the interaction between the plates is nonpairwise additive. Interestingly this makes it possible to describe the system in terms of bullk and surface free energies,

$$\Delta F_0^N = N f_{\text{bulk}} + f_{\text{surface}} + O(N^{-1}), \quad N\to\infty, \quad (6)$$

where f_{bulk} and f_{surface} are, the bulk and surface free energies, given by

$$f_{\text{bulk}} \sim -k_B T h^{-2},$$

$$f_{\text{surface}} \sim k_B T h^{-2}, \quad (7)$$

respectively, note that both f_{bulk} and f_{surface} are larger in magnitude at high temperatures.

If we calculated the free energy by summing over all pairs of plates using the two-body long-wavelength interaction given in Eq. (4), then we would obtain a free energy given as follows:

$$\Delta F_{\text{pairwise}}^N \sim k_B T(-N+\log N)h^{-2}, \quad N\to\infty. \quad (8)$$

It is tempting to identify the first and second terms as bulk and surface free energies respectively. In a strict sense, however, this calculation does not lead to a well-defined surface free energy. Thus the breakdown of pairwise additivity ensures the existence of the thermodynamic limit in this system. Also the free energy calculated explicitly is more negative than that based on the assumption of pairwise additivity for large N. In fact, charges are more efficiently correlated in the explicit calculation, resulting in a lower free energy.

At low temperatures, however, the interactions between the plates are dominated by SW charge fluctuations. In this case, only the nearest pairs of the plates couple strongly, and thus the resulting interactions are approximately pairwise additive. Consequently both the bulk and surface free energies vary as $e^{-2k_\perp^> h}$. It is obvious that the magnitudes of these terms are larger at low T.

IV. CHARGE CORRELATIONS

The appearance of two distinctive competing interactions, i.e., F_{LW} and F_{SW}, can also be understood in terms of in-plane charge correlations for a single plate: $G_1(\mathbf{r}_\perp,\mathbf{r}'_\perp)=\langle\hat{\sigma}(\mathbf{r}_\perp)\hat{\sigma}(\mathbf{r}'_\perp)\rangle-\langle\hat{\sigma}(\mathbf{r}_\perp)\rangle\langle\hat{\sigma}(\mathbf{r}'_\perp)\rangle$. The long-wavelength contribution to the charge correlation was shown to scale as $G_{\text{LW}}(\mathbf{r}_\perp,r'_\perp)\sim -k_B T/|\mathbf{r}_\perp-\mathbf{r}'_\perp|^3$ for large $|\mathbf{r}_\perp-\mathbf{r}'_\perp|$ [33]. Note that this correlation vanishes as $T\to 0$. Our result in Eq. (2)

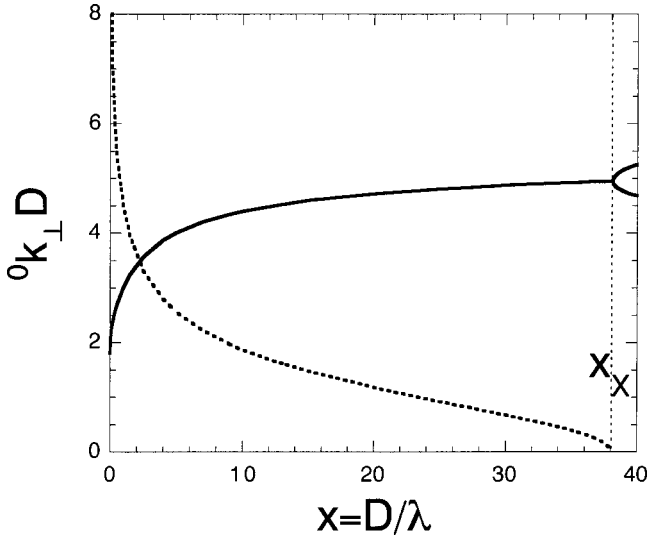

FIG. 3. The leading poles ${}^0k_\perp$ as a function of $x \equiv D/\lambda$. The solid and dotted lines correspond to the real and imaginary parts respectively. At x_X (corresponding to $\lambda^{-1}=\lambda_X^{-1}\simeq 7.6\ \text{Å}^{-1}$), marked by the vertical dotted line, the correlation is no longer damped, and the system crystallizes.

implies that the short-wavelength charge correlation function is given by

$$G_{SW}(\mathbf{r}_\perp,\mathbf{r}_\perp')\simeq\sigma_0 g(\mathbf{r}_\perp,\mathbf{r}_\perp')-\frac{\sigma_0 e^2}{2\pi}\times\int_{k_\perp\neq{}^0}\frac{k_\perp dk_\perp g(\mathbf{k}_\perp)}{1+\dfrac{\lambda k_\perp}{g(k_\perp)}}J_0(k_\perp|\mathbf{r}_\perp-\mathbf{r}_\perp'|), \quad (9)$$

where $J_0(x)$ is the zeroth-order Bessel function of the first kind. Unlike $G_{\rm LW}(\mathbf{r}_\perp,\mathbf{r}_\perp')$, $G_{\rm SW}(\mathbf{r}_\perp,\mathbf{r}_\perp')$ is determined by the nature of the poles of $[1+\lambda k_\perp/g(\mathbf{k}_\perp)]^{-1}$ (note that $J_0(x)\sim\sqrt{2/\pi x}\cos[x-(\pi/4)]$ for large x.).

In order to analyze the leading behavior of $G_{\rm SW}$, we find the pole ${}^0k_\perp$ that is closest to the origin in the complex $k_\perp$ plane. We have plotted the results in Fig. 3 as functions of $x\equiv D/\lambda$. Notably, our results in Fig. 3 imply that $G_{\rm SW}$ shows an oscillatory decay; the real part of ${}^0k_\perp$, denoted by $\mathrm{Re}^0 k_\perp$, which controls the wavelength of the oscillation, is described by a solid line, while the imaginary part, which sets the decay length, is a dotted line. Note that $\mathrm{Re}^0 k_\perp$ is essentially equal to $k_\perp^>$ in the limit of $h\to\infty$. As x (thus λ^{-1}) increases, the wavelength of the oscillation decreases, while the decay length increases. At $x=x_X\simeq 38$ or $\lambda^{-1}=\lambda_X^{-1}\simeq 7.6\ \text{Å}^{-1}$ [32], marked by a vertical dotted line, the imaginary part vanishes and the decay length diverges, signaling the onset of crystallization of the counterions. The temperature dependence of the amplitude of the charge correlation can be estimated in the same spirit as in the short-wavelength plate interaction. We find that this amplitude varies as $T^{-1}[1+(\mathrm{Re}^0 k_\perp)^{-1}\lambda^{-1}g(\mathrm{Re}^0 k_\perp)]^{-1}$ and is larger at low temperatures.

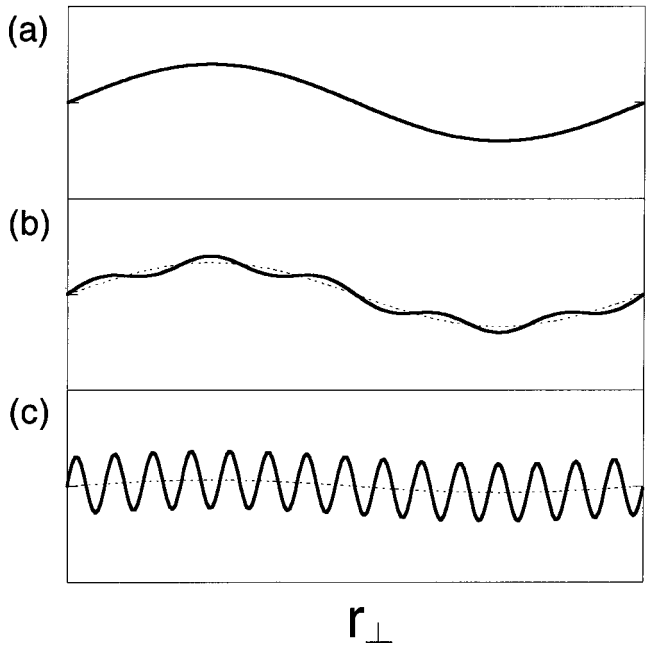

FIG. 4. One-dimensional illustration of typical fluctuations in the counterion density. The thin dotted lines are to guide the eye. (a) At high temperatures, LW fluctuations are dominant over SW fluctuations, leading to power-law pressures. (b) Near the crossover boundaries, both LW and SW fluctuations contribute to the free energy. Within each counterion-rich or-poor domain, counterions tend to develop local positional ordering. Due to the presence of many competing length scales, the electrostatic pressure in this case does not assume a simple scaling form. (c) At low temperatures, however, SW fluctuations are dominant, as characterized by oscillatory charge correlations. There is thus strong cancellation between repulsions with attractions, leading to an exponentially decaying pressure.

At high temperatures, LW fluctuations are dominant [a typical mode of LW fluctuations is illustrated in Fig. 4(a)], and thus we can consider each plate to consist of large domains, i.e., counterion-rich and counterion-poor domains. The size of the domains is on the order of $(k_\perp^<)^{-1}\gg 1$ Å, and thus these domains can form huge dipoles, as manifested by power-law correlations. This results in a long-ranged attraction between charged surfaces. The long-wavelength fluctuations couple over many plates, leading to breakdown of pairwise additivity [34]. Near the crossover boundary, SW and LW fluctuations are equally important, as schematically shown in Fig. 4(b).

In contrast, each domain at low temperature becomes overall charge neutral, and thus the distinction between domains is meaningless. In this case, the local correlation between a counterion and a backbone charge in its neighborhood dominates the free energy, as illustrated in Fig. 4(c). There is thus strong cancellation of repulsions (between like charges), with attractions (between opposite charges). This results in an exponentially decaying, short-ranged attraction between the plates.

V. CONCLUSIONS

In conclusion, we have introduced a model for describing counterion-mediated attractions between fluid membranes.

We have shown that our model can capture the essential features of these attractions at both high and low temperatures. At high temperatures, these interactions are dominated by LW fluctuations, and are long ranged and nonpairwise additive. Charge densities of biomembranes range from $-0.03e/\mathrm{nm}$ to $-0.24e/\mathrm{nm}^2$, corresponding to LW regimes at room temperature; two adjacent lipid head groups are separated by a distance between 20 and 60Å, much larger than the Bjerrum length, and the positional ordering between the lipids and their counterions can easily be perturbed by thermal fluctuations. In order for crossover to take place at room temperature for the case $Z=2$ and $D=5$ Å, two adjacent charged lipids should be within a length 5Å [35], which is somewhat smaller than the typical size of lipid heads (~ 8 Å). Many-body, nonpairwise additive interactions thus operate between charged membranes at room temperature unless the counterion valency is too large.

In contrast, the membrane interactions at low temperatures are dominated by SW charge fluctuations. The resulting interactions are pairwise additive, and decay exponentially with the membrane spacing (the nonpairwise additive interaction becomes smaller, and eventually vanishes, as $T\rightarrow 0$). The approach presented here allows one to systematically study the crossover, as the temperature decreases, from the high-temperature, long-ranged attractions to the behaviors expected at low temperatures.

In our theoretical approach, the nonzero ionic size plays a significant role in ensuring finite charge separations (thus to avoid collapse of the system) at $T=0$. We can also imagine a system of one type of ions pinned to lattice sites, with mobile counterions of a different valency. In this case, this effect is not needed to ensure finite charge separations at $T=0$. In our theoretical scheme, we assume that the membrane charges are also mobile in the plane of the membrane surface, consistent with our conception of membranes as a two-dimensional fluid, and the finite ionic size is certainly needed to avoid collapse at $T=0$. The significance of the finite ionic size is further illustrated in Appendix B. Our model is also different from a system of point charges localized to a uniform neutralizing surface, the so called Wigner crystal model. It was shown [27] that a finite size of the ions is not required in this model to ensure a nonvanishing attraction at $T=0$. This model is similar to the case of pinned charges in that the background charges are *quenched*. If the background charges were allowed to relax in response to their counterions, then this system would collapse onto a point at $T=0$ as a two-dimensional ionic fluid does.

Despite this apparent distinction, all these models, including ours, rely on an assumption that prevents the system from collapsing onto a point at $T=0$. In the case of a fluid membrane, it is certainly the ionic size that prevents the collapse. In the case of quenched backbone charges, this collapse can be prevented by a constraint enforced on the backbone charges; the backbone charges do not respond to any change in temperature and counterions. No matter what model is used, however, the exponentially decaying pressure is a generic feature of the electrostatic attraction between like-charged surfaces at low temperatures, even though the temperature dependence of this attraction and thus crossover conditions are model-specific, as argued in Appendix A. Thus all these models lead to a qualitatively similar picture for the attraction.

Counterion-mediated attractions play a key role in such physical and biophysical processes as membrane adhesion, packaging of DNA into a compact bundle, and aggregation of charged colloids. Due to the simultaneous presence of a long-ranged repulsion, arising from the net charge carried by DNA, and an attraction induced by counterions, there is a free energy barrier to bundle growth [36]. As it turns out, this barrier essentially determines the size (i.e., the cross sectional diameter) of DNA bundles in the case of DNA packaging. In colloidal systems, this barrier can stabilize the system against coagulation. Both the height and location of the barrier can be sensitive to the dominant modes of charge fluctuations (i.e., either LW or SW fluctuations), since different modes induce different types of attractions. So far we have restricted ourselves to the case of no added salts. Our theoretical scheme can readily be generalized to the case of added salts as in real biological settings. We leave the study of salt effects on the aggregational behaviors of macroions for future work.

ACKNOWLEDGMENTS

We have benefited from illuminating discussions with A. W. C. Lau and A. J. Liu. We thank W. M. Gelbart, H. Schiessel, and R. Menes for scientific stimulation, M. Howard for reading the manuscript carefully, and D. Boal, M. Wortis, and M. Plischke for their hospitality. This work was supported by the NSERC of Canada.

APPENDIX A

In this appendix, we argue that the electrostatic attraction between two like-charged parallel plates a distance h apart decay exponentially with h as long as in-plane charge correlations exhibit oscillatory decays. This can be most readily seen in perturbative evaluations of the attraction. To this end, we write the interaction Hamiltonian for the two-plate system as

$$\mathcal{H}_2=\mathcal{H}_{11}+\mathcal{H}_{22}+2\mathcal{H}_{12}, \tag{A1}$$

where $\mathcal{H}_{ij}$ refers to the interactions between charges on plate i and j, i.e.,

$$\mathcal{H}_{ij}=\frac{1}{2\epsilon}\int\int d\mathbf{r}_\perp d\mathbf{r}'_\perp \frac{\hat{\sigma}_i(\mathbf{r}_\perp)\hat{\sigma}_j(\mathbf{r}'_\perp)}{\sqrt{(\mathbf{r}_\perp-\mathbf{r}'_\perp)^2+h_{ij}^2}}, \tag{A2}$$

where $h_{ii}=0$ and $h_{i\neq j}=h$. When the separation between the plates is somewhat larger than the average distance between two adjacent charges on the same plate, we can consider $\mathcal{H}_{12}$ as a perturbation. In this case, the free energy can be expanded as

$$\Delta\mathcal{F}_2\simeq\frac{2}{k_BT}\langle\mathcal{H}_{12}^2\rangle+\mathcal{O}(\mathcal{H}_{12}^4)+\mathrm{const}, \tag{A3}$$

where const refers to h-independent terms. The leading term in $\Delta\mathcal{F}_2$ can be written in terms of the in-plane charge correlation $G(\mathbf{r}_\perp,\mathbf{r}'_\perp)$ introduced in Sec. IV,

$$\langle \mathcal{H}_{12}^2\rangle = \frac{k_BT}{\lambda^2}\int\int\int\int d\mathbf{r}_\perp d\mathbf{r}'_\perp d\mathbf{r}''_\perp d\mathbf{r}'''_\perp \times \frac{G(\mathbf{r}_\perp,\mathbf{r}''_\perp)}{\sqrt{(\mathbf{r}''_\perp-\mathbf{r}'''_\perp)^2+h^2}}\frac{G(\mathbf{r}'''_\perp,\mathbf{r}'_\perp)}{\sqrt{(\mathbf{r}'_\perp-\mathbf{r}_\perp)^2+h^2}} = \frac{k_BT}{\lambda^2}\sum_{k_\perp}|G(\mathbf{k}_\perp)|^2\frac{e^{-2\mathbf{k}_\perp h}}{k_\perp^2}, \tag{A4}$$

where $G(\mathbf{k}_\perp)$ is the Fourier transform of $G(\mathbf{r}_\perp,\mathbf{r}'_\perp)$.

When the in-plane charge correlation is dominated by an oscillatory decay (with the wavelength $2\pi/k_\perp^>$), $G(\mathbf{k}_\perp)$ has a sharp peak at $k_\perp^>$. In this case, the interaction between the two plates is well approximated by the leading terms (high-order terms decay faster). Up to an h-independent constant, the two-plate interaction per unit area is

$$\Delta F_2 \simeq -k_BTf(T)\frac{e^{-2k_\perp^> h}}{\lambda^2 k_\perp^2}, \tag{A5}$$

where we subsummed h-independent factors into $f(T)$, which is a function of T. This result is illuminating; the exponentially decaying attraction is a generic (model-independent) feature of the electrostatic attraction between like-charged surfaces at low temperatures where the in-plane charge correlation oscillates. The temperature dependence of this attraction and thus crossover conditions are, however, model specific.

APPENDIX B

Our theoretical scheme relies on the finite size of ions. In this appendix, we further illustrate the significance of this effect in ensuring finite charge separations at low temperatures. To this end, we consider an ionic fluid consisting of negative charges and neutralizing counterions of valency Z confined to a plane, as a model of a highly negatively charged fluid membrane with the surrounding counterions. Most of crucial properties of this system can be derived by holding any particular ion and examining how the other particles respond. Since the system is electrically neutral, each ion should create around itself an ionic cloud of the opposite charge. To be specific, we put a counterion at the origin and examine the electric potential created by this ion and the surrounding ionic cloud, denoted by $Z\Psi(\mathbf{r})$. The counterion is assumed to be a hard sphere of diameter D, excluding other ions for $r_\perp<D$. Note that this is a two-dimensional analog of the so called restricted primitive model (RPM) [37].

If the plane of the ionic fluid is at $z=0$. the electrostatic potential at $(\mathbf{r}_\perp,z)$, in the linearized Poisson-Boltzmann or Debye-Hückel approach, satisfies

$$e\nabla^2\Psi(\mathbf{r}) = \begin{cases} 0, & \text{for } 0<r_\perp\leqslant D \\ \dfrac{2}{\lambda}\Psi(\mathbf{r})\delta(z), & \text{for } r_\perp>D. \end{cases} \tag{B1}$$

Here we are particularly interested in the electric potential in the plane of the surface, $\psi(\mathbf{r}_\perp)\equiv\Psi(\mathbf{r}_\perp,z)$, since this will essentially determine in-plane charge separations. To understand low-T properties of $\psi(\mathbf{r}_\perp)$, note that $\lambda^{-1}\to\infty$ as $T\to 0$. Since $\psi(\mathbf{r}_\perp)$ is a continuous function of $\mathbf{r}_\perp$, the left hand side of Eq. (B1) should be finite. This requires that, for $r_\perp>D$, $\psi(\mathbf{r})\to 0$ as $T\to 0$. Thus the counterion charge is thus more efficiently shielded by the ionic cloud at low temperatures. In fact, it has been shown that, for $r_\perp>D$, $\psi(\mathbf{r}_\perp)$ is given by [38]

$$\psi(\mathbf{r}_\perp) = -\left(\frac{eZ}{\epsilon r_\perp}\right)\left(\frac{\lambda}{D}\right)\frac{1-\dfrac{\pi}{2\pi}\left(\dfrac{r_\perp}{\lambda}\right)\left[H_0\left(\dfrac{r_\perp}{\lambda}\right)-Y_0\left(\dfrac{r_\perp}{\lambda}\right)\right]}{\left\{1-\dfrac{\pi}{2\pi}\left[H_1\left(\dfrac{D}{\lambda}\right)-Y_1\left(\dfrac{D}{\lambda}\right)\right]\right\}}, \tag{B2}$$

where $H_v(x)$ is the Struve function, and $Y_v(x)$ is the Bessel function of the second kind. For the case of $D=0$, $\psi(\mathbf{r}_\perp)/T$ decays as T/r^3 as $T\to 0$. This implies that the charge correlation decays linearly with decreasing T, reminiscent of vanishing charge fluctuations at $T=0$.

Charge separations or charge fluctuations can be quantified in terms of multipoles. For example, the mean square of the electric dipole produced by charge fluctuations is given by

$$\mu^2 = \int\int d\mathbf{r}_\perp d\mathbf{r}'_\perp \mathbf{r}_\perp\mathbf{r}'_\perp\langle\hat\sigma(\mathbf{r}_\perp)\hat\sigma(\mathbf{r}'_\perp)\rangle. \tag{B3}$$

Thus the magnitude of μ^2 is directly related to the charge correlation: $\langle\hat\sigma(\mathbf{r}_\perp)\hat\sigma(\mathbf{r}'_\perp)\rangle$. Note here that the contribution from $\mathbf{r}_\perp=\mathbf{r}'_\perp$ is omitted in the integral. Equations (B2) and (B3) imply that the electric dipole decreases to zero as $T\to 0$. In the Debye-Hückel approach, which retains fluctuations at the Gaussian level, it is straightforward to show that all higher multipoles vanish at $T=0$. This follows from the fact that any N-point correlation function (N must be even) is represented as a sum of all possible product of two-point functions, i.e., Wick's theorem. In the Debye-Hückel approach, charge separations are thus completely suppressed at $T=0$ to all orders.

When a second plate is brought close to the plate, these in-plane charge fluctuations are felt by the second plate, as also implied by Eq. (A4)—the charge distribution on one plate is complementary to that on the second plate. As $T\to 0$, all multipoles induced by charge fluctuations vanish. At finite temperatures, they essentially lead to the LW contribution to the charge fluctuation free energy F_{LW}.

For $D>0$, however, $\psi(\mathbf{r}_\perp)/k_BT$ approaches a finite value: $\lim_{T\to 0}\psi(\mathbf{r}_\perp)/k_BT\to 1/2\pi\epsilon e^2\sigma_0(1+Z)$. This implies that, for $D>0$, charge fluctuations do not vanish at $T=0$. This model, however, suffers from a serious deficiency: it does not predict an oscillatory charge correlation at low tempera-

tures that essentially leads to an exponentially decaying pressure for the case of two plates. So the resulting model, i.e., the two-dimensional RPM cannot be used to study the crossover between the power-law pressure and the exponentially decaying one, though this is certainly an improvement on the two-dimensional Debye-Hückel theory for point charges.

Finite charge separations (thus a nonvanishing attraction) are ensured as soon as the nonzero ionic size is incorporated via the two-dimensional form factor $g(\mathbf{r}_\perp,\mathbf{r}'_\perp)$. The linearized PB equation in this case for $r_\perp > D$ should read

$$e\nabla^2\Psi(\mathbf{r}) = \frac{2}{\lambda}\int d\mathbf{r}'_\perp \Psi(\mathbf{r}'_\perp, \quad z=0) g(\mathbf{r}_\perp - \mathbf{r}'_\perp). \quad \text{(B4)}$$

For $r_\perp > D$, we find

$$\psi(\mathbf{r}_\perp) = \frac{A}{r_\perp} - \frac{\lambda^{-1}}{2\pi}\int\int d\mathbf{r}'_\perp d\mathbf{r}''_\perp \frac{\psi(\mathbf{r}'_\perp) g(\mathbf{r}'_\perp - \mathbf{r}''_\perp)}{|\mathbf{r}_\perp - \mathbf{r}'_\perp|}. \quad \text{(B5)}$$

The solution of this equation is given by

$$\psi(\mathbf{r}_\perp) = A\int dk_\perp \frac{e^{-i\mathbf{k}_\perp\cdot\mathbf{r}_\perp}}{1+\dfrac{g(k_\perp)}{\lambda k_\perp}}. \quad \text{(B6)}$$

In principle, the integration constant A can be determined by requiring that the system is electric neutral. Except for $g(\mathbf{k}_\perp)=1$, it is, however, formidable to implement this requirement. Nevertheless, it can be shown that $\psi(\mathbf{r}_\perp)$ in the case of $g(k_\perp)\neq 1$ does not have to vanish in the limit of $T\to 0$. To this end, first note that the zero-$k_\perp$ component of $\psi(\mathbf{k}_\perp)$ decreases as the temperature is lowered, and vanishes at $T=0$—note that short-range correlations are not ''felt'' by zero-$k_\perp$ fluctuations. In contrast, large-$k_\perp$(or SW) components of $\psi(\mathbf{r}_\perp)$ do not have to decrease as the temperature is lowered, since $g(\mathbf{k}_\perp)$ can take negative values; in this case, smaller λ (i.e., low T) can correspond to a large amplitude of $\psi(\mathbf{k}_\perp)$. This implies that $\psi(\mathbf{r}_\perp)$ can be larger at low temperatures. In this paper, we relax the requirement that ions are excluded for $r_\perp > D$. This relaxation amounts to requiring that $A = Ze/\epsilon$ and so this approximation does not change the underlying physics qualitatively, since this will modify the free energy in Eq. (2) by an overall multiplicative prefactor. None of our core results described by the phase diagram in Fig. 2 or the leading poles in Fig. 3 are influenced by this approximation.

[1] B.-Y. Ha and A. J. Liu, Phys. Rev. Lett. **79**, 1289 (1997).
[2] B.-Y. Ha and A. J. Liu, Phys. Rev. Lett. **81**, 1011 (1998).
[3] N. Grønbech-Jensen, R. J. Mashl, R. F. Bruinsma, and W. M. Gilbart, Phys. Rev. Lett. **78**, 2477 (1997).
[4] J. L. Barrat and J. F. Joanny, Adv. Chem. Phys. **94**, 1 (1996).
[5] V. A. Bloomfield, Biopolymers **31**, 1471 (1991); Curr. Opin. Struct. Biol. **6**, 334 (1996), and references therein.
[6] S. M. Klimenko, T. I. Tikchonenko, and V. M. Andreev, J. Mol. Biol. **23**, 523 (1967).
[7] J. X. Tang, S. Wong, P. Tran, and P. Jammey, Ber. Bunsenges. Phys. Chem. **100**, 1 (1996); J. X. Tang, T. Ito, T. Tao, P. Traub, and P. A. Janmey, Biochemistry **36**, 12 600 (1997), and references therein.
[8] M. Kardar and R. Golestanian, Rev. Mod. Phys. **71**, 1233 (1999).
[9] P. A. Pincus and S. A. Safran, Europhys. Lett. **42**, 103 (1998).
[10] D. B. Lukatsky and S. A. Safran, Phys. Rev. E **60**, 5848 (1999).
[11] N. Lee and D. Thirumalai, e-print cond-mat/9907199; e-print cond-mat/0001094.
[12] J. N. Israelachvili and P. M. McGuiggan, Science **241**, 795 (1988); D. E. Leckband, C. A. Helm, and J. Israelachvili, Biochemistry **32**, 1127 (1993).
[13] B.-Y. Ha, Phys. Rev. E (to be published).
[14] S. Marcelja, Biophys. J. **61**, 1117 (1992).
[15] G. S. Manning, J. Chem. Phys. **51**, 954 (1969).
[16] F. Oosawa, Biopolymers **6**, 134 (1968); Polyelectrolytes (Dekker, New York, 1971).
[17] I. Rouzina and V. A. Bloomfield, J. Phys. Chem. **100**, 9977 (1996).
[18] J. J. Arenzon, J. F. Stilck, and Y. Levin, Eur. Phys. J. B **12**, 79 (1999); Y. Levin, J. J. Arenzon, and J. F. Stilck, Phys. Rev. Lett. **83**, 2680 (1999).
[19] F. J. Solis and M. O. de la Cruz, Phys. Rev. E **60**, 4496 (1999).
[20] A. A. Korynshev and S. Leikin, J. Chem. Phys. **107**, 3656 (1997); Biophys. J. **75**, 2513 (1998).
[21] B. I. Shklovskii, Phys. Rev. Lett. **82**, 3268 (1999).
[22] B.-Y. Ha and A. J. Liu, Phys. Rev. E **58**, 6281 (1998).
[23] B.-Y. Ha and A. J. Liu, Phys. Rev. E **60**, 803 (1999).
[24] B.-Y. Ha and A. J. Liu, Phys. Rev. Lett. **83**, 2681 (1999).
[25] A. W. C. Lau, D. Levine, and P. Pincus, Phys. Rev. Lett. **84**, 4116 (2000).
[26] R. Podgornik and V. A. Parsegian, Phys. Rev. Lett. **80**, 1560 (1998).
[27] At the end of this work, we became aware of a preprint by A. W. Lau, P. Pincus, and D. Levine, in which a similar issue was considered.
[28] An alternative, complementary approach could be to perturb around the ionic crystal. However, this may fail to capture strong fluctuations at high T [27], just as our approach does not accurately describe charge correlations near and below the freezing transition.
[29] This, however, does not limit the validity of our theory. This is because, near and at the crossover boundary (i.e., at low temperatures), the contribution of the delocalized counterions to the plate-plate interaction is negligible—most of counterions are localized to one of the plates. On the other hand, short-wavelength fluctuations disappear at high temperatures. This enables us to discuss the crossover from the $1/h^3$ pressure to the exponentially decaying one independently of the competition between the two types of algebraically decaying pressures: $1/h^3$ and $1/h$ pressures. The discussion of the latter requires an

involved numerical analysis of the spatial distribution of counterions, as implied by the nonlinear Poisson-Boltzmann (PB) equation, and counterion-density fluctuations around the PB solution [30].

[30] A. Sain and B.-Y. Ha (unpublished).

[31] In this calculation, surface charges and their counterions are assumed to be in the same plane.

[32] Note that this value is somewhat larger than the corresponding value for two plates, i.e., $\lambda_X^{-1} \simeq 7.2\ \text{Å}^{-1}$.

[33] P. Attard, D. J. Mitchell, and B. W. Ninham, J. Chem. Phys. **88**, 4987 (1988).

[34] For a similar issue in rodlike systems, see Ref. [22].

[35] This number corresponds to $h=0$. More realistically, we may assume that two plates cannot approach each other more closely than a minimum separation $h_{\min} \simeq D$. Then the crossover takes place for a higher charge density than implied by this number.

[36] B.-Y. Ha and A. J. Liu, Europhys. Lett. **46**, 624 (1999).

[37] See, for example, D. A. McQuarrie, *Statistical Mechanics* (Harper and Row, New York, 1971), Chap. 15.

[38] E. S. Velázquez and L. Blum, Physica A **244**, 453 (1997).